# Supplementary Information

## Strain-durable and stretchable electrodes with low interfacial impedance using liquid metal/PEDOT:PSS fiber mat for multifunctional epidermal bioelectronics

Fuqin Wu,[a] Pengmin Liu,[a] Junhan Li,[b] Wenjing Guo,[a] Xiaotong Wang,[c] Ruifang Guan,[a] Duxia Cao,*[a] Songfang Zhao,*[a] Yongju Gao,*[d] Yang Li,[e] William W. Yu,*[f]

[a]School of Materials Science and Engineering, University of Jinan, Jinan 250022, China. E-mail: duxiacao@ujn.edu.cn, zhaosongfang@163.com,

[b]School of Information Science and Engineering, University of Jinan, Jinan 250022, China

[c]Qingdao Eco-environment Monitoring Center of Shandong Province, Qingdao 266003, China

[d]Shandong Zhongke Advanced Technology Co., Ltd., Jinan 250000, China. E-mail: 416038@163.com

[e]School of Microelectronics Shandong University, Jinan 250101, China

[f]School of Chemistry and Chemical Engineering, Shandong University, Jinan 250100, China. E-mail: wyu6000@gmail.com

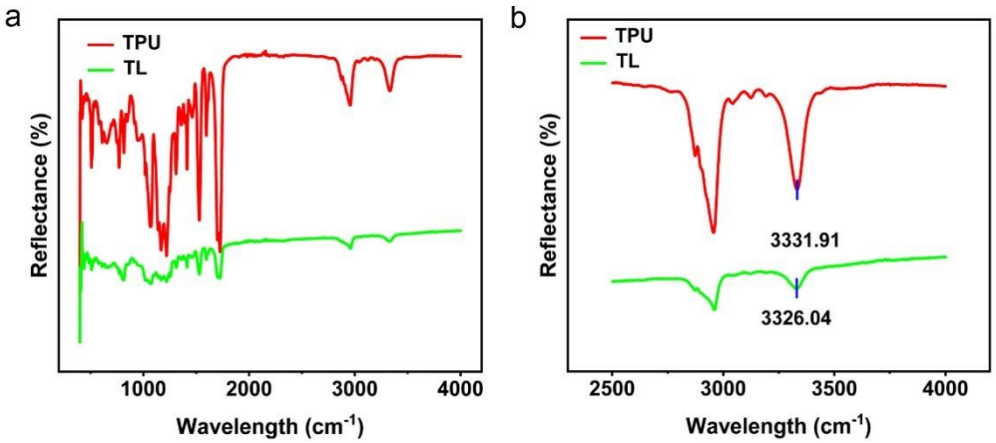


**Fig. S1** Fourier transform-infrared spectra of different samples.

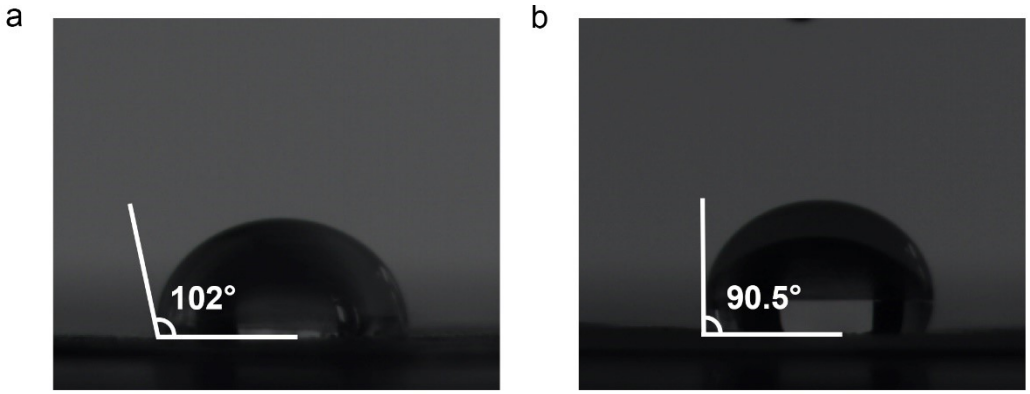


**Fig. S2** Contact angles of LM on different fibrous mats: (a) TPU fibrous mat, (b) SBS fibrous mat.

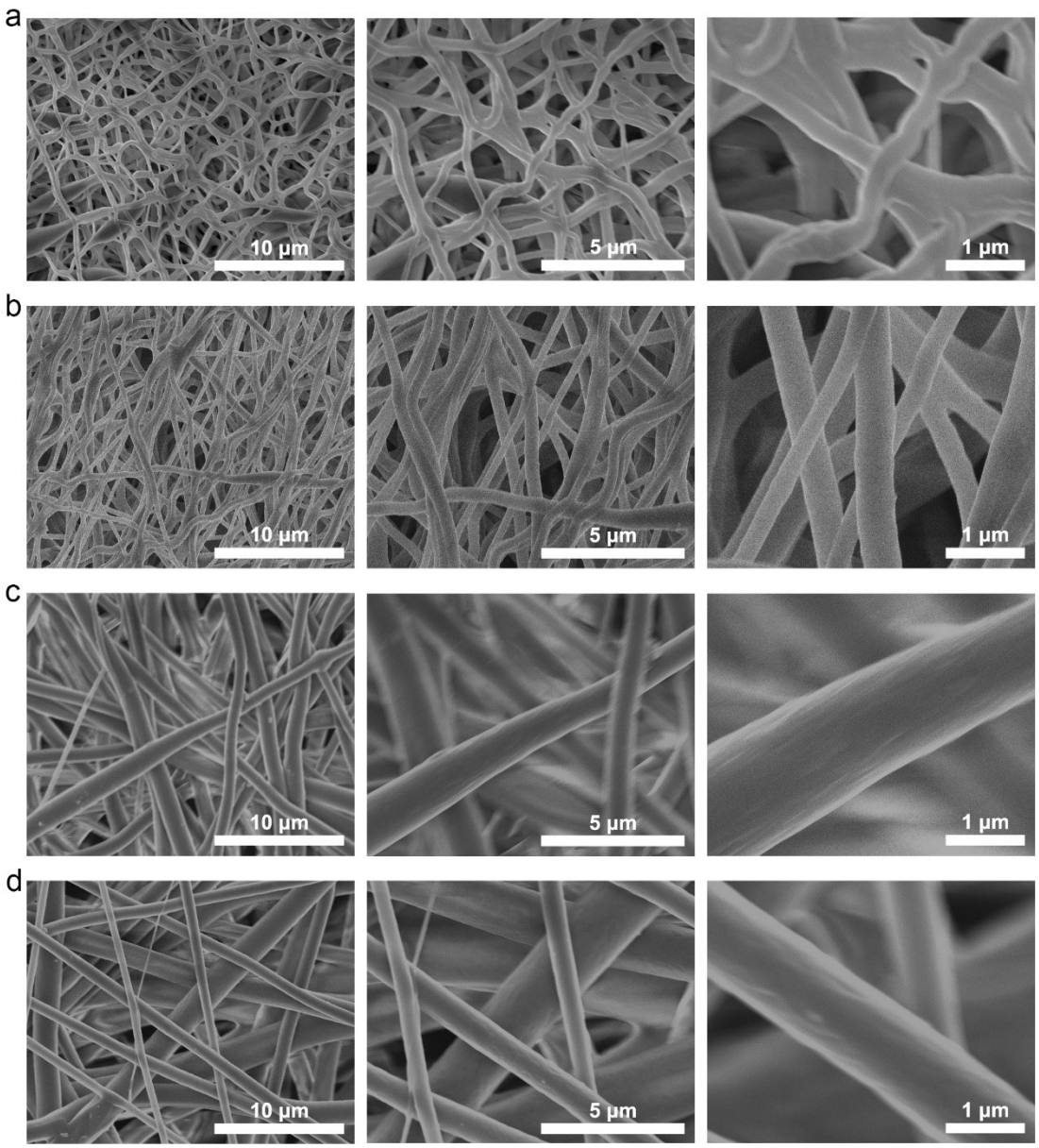


**Fig. S3** SEM images of TPU fibers at different magnifications: (a) 10% TPU, (b) 13% TPU, (c) 15% TPU, (d) 18% TPU.

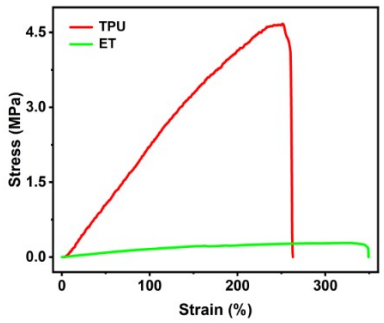


**Fig. S4** Stress-strain curves of the electrospun TPU film and the ET film.

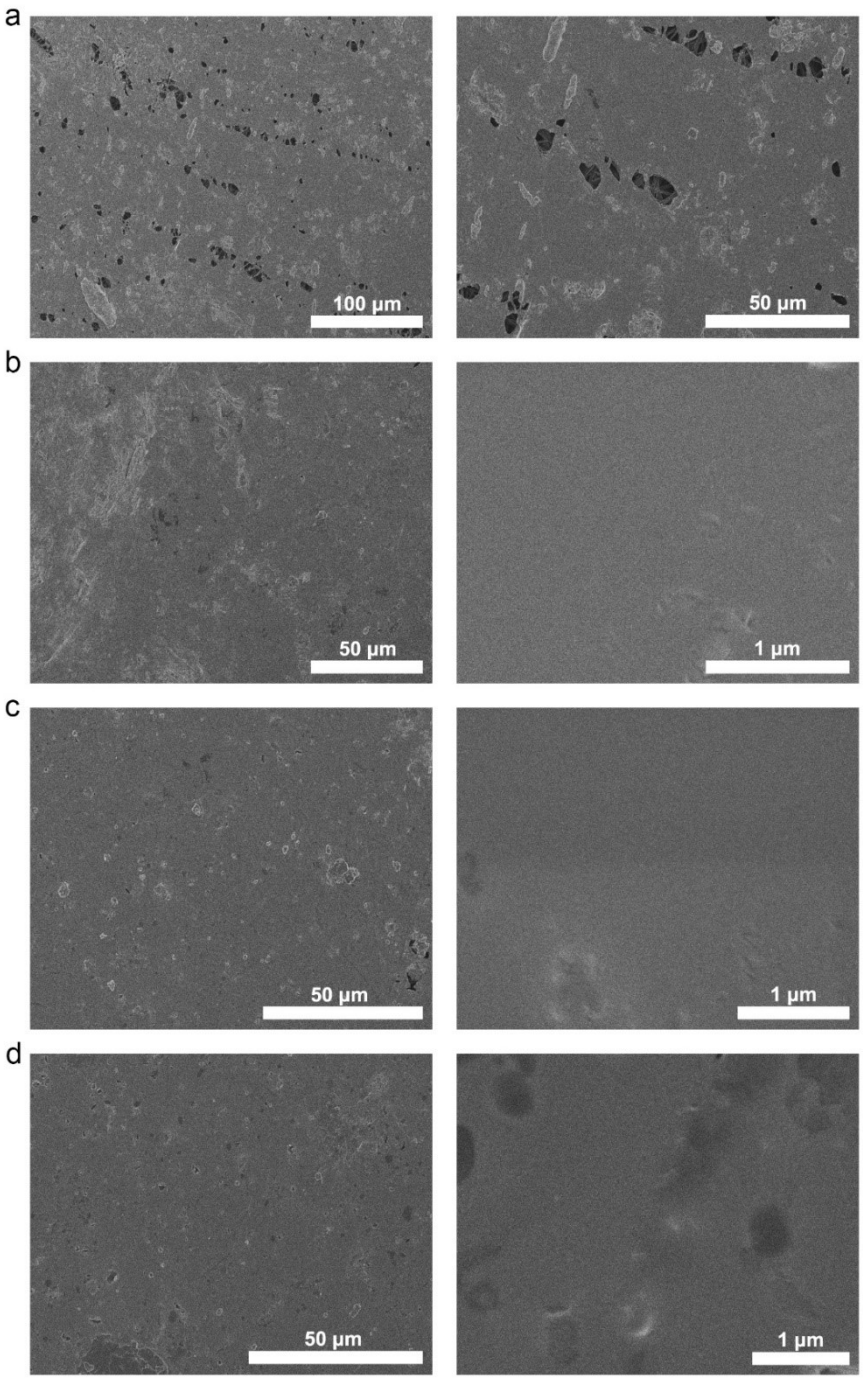


**Fig. S5** SEM images of ETL films coated with different amount of LM: (a) 1.2 mg $cm^{-2}$, (b) 2.0 mg $cm^{-2}$, (c) 2.8 mg $cm^{-2}$, (d) 3.6 mg $cm^{-2}$.

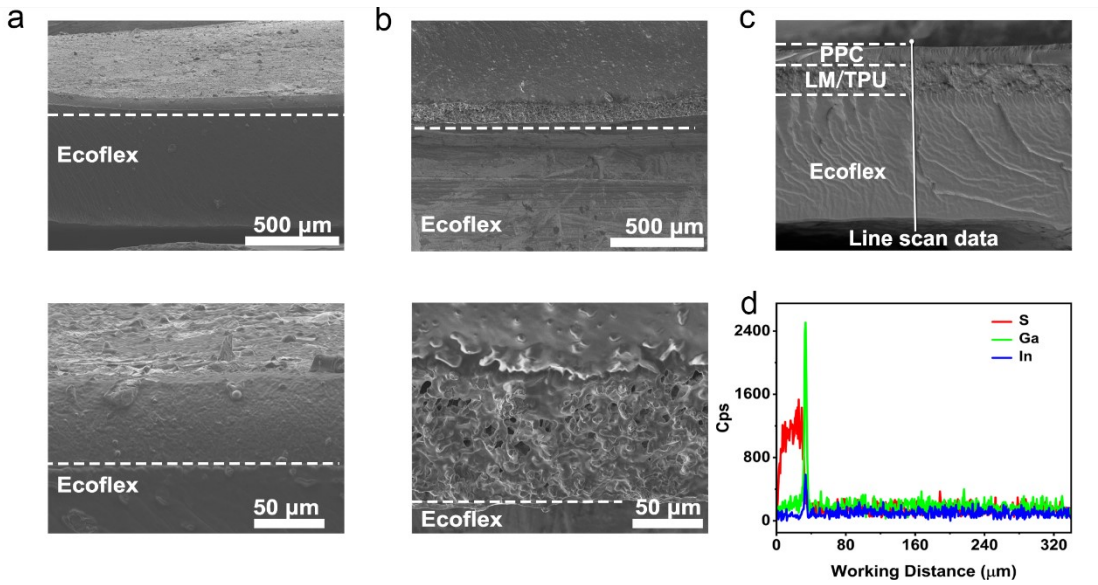


**Fig. S6** (a) Cross-sectional SEM images of ETL, (b) Cross-sectional SEM images of ETLP, (c) SEM image of the ETLP electrode cross-section, (d) Line-scan EDS elemental distribution profiles corresponding to Line across the cross-section of the ETLP electrode.

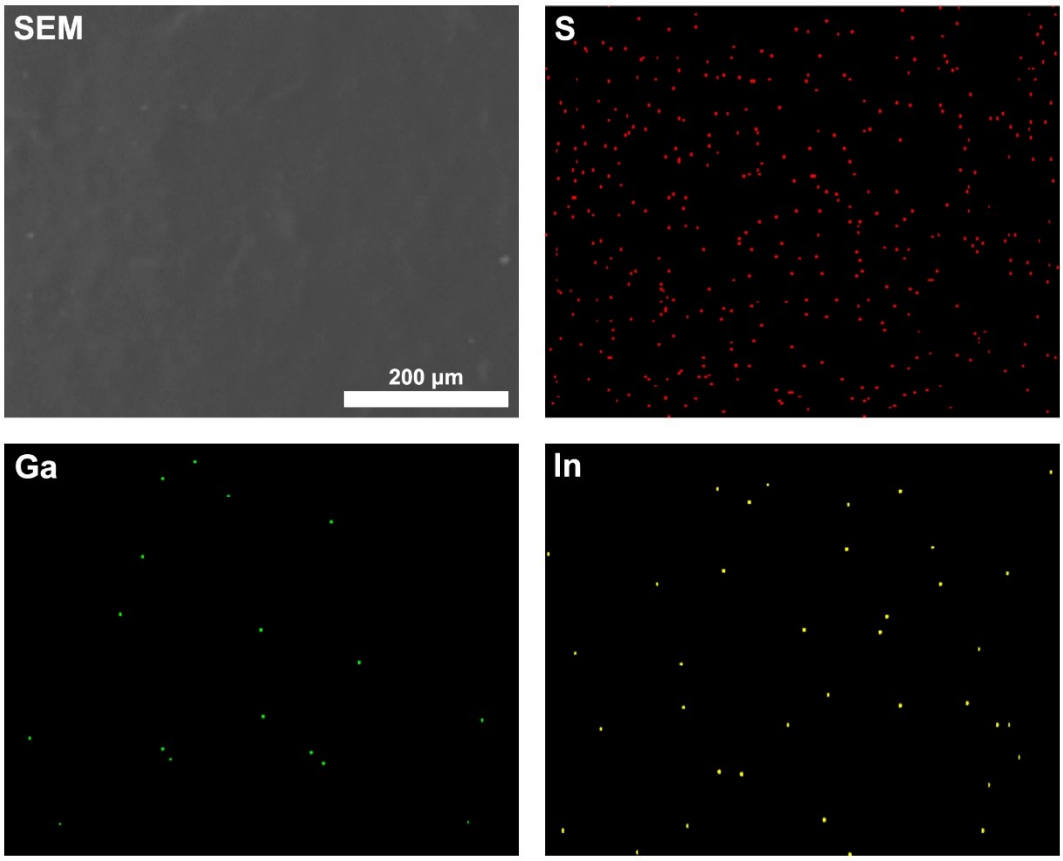


**Fig. S7** EDS spectrum of the ETLP film.

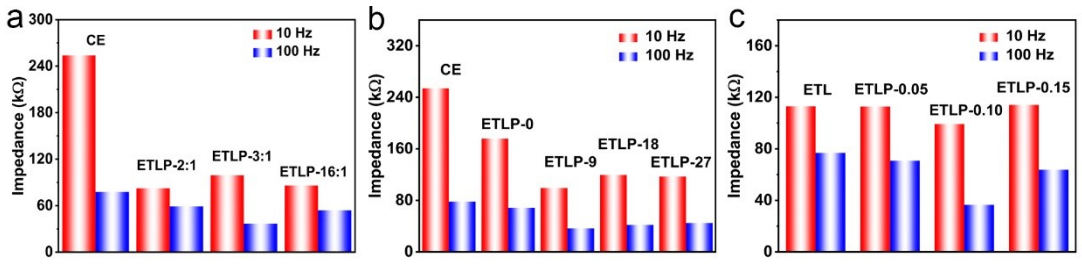


**Fig. S8** Interfacial impedance measured at 10 Hz and 100 Hz: (a) Interfacial impedance with different $V_{PEDOT:PSS}/V_{PVA}$ ratios; (b) Interfacial impedance with varied CA mass; (c) Interfacial impedance at different coating volumes of 0.10-0.15 mL.

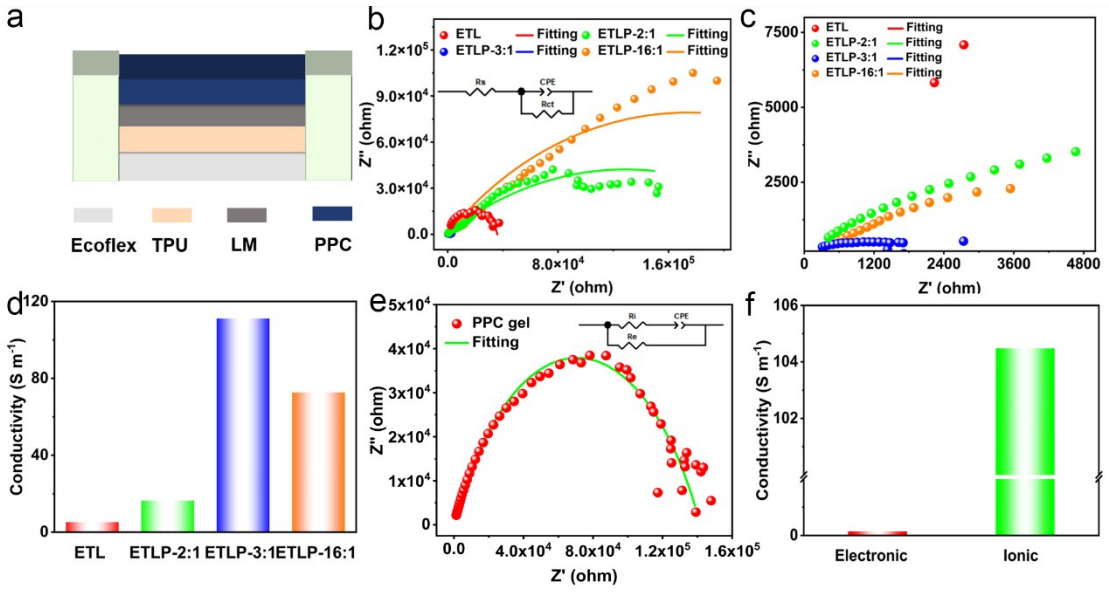


**Fig. S9** (a) Schematics of ETLP electrodes connected with external circuit. (b) Nyquist plots of ETLP electrodes with different $V_{PEDOT:PSS}$:$V_{PVA}$ ratios. (c) Enlarged Nyquist plots. (d) Comparison of conductivity of different electrodes. (e) Nyquist plot of PPC gel. (f) Comparison of ionic and electronic conductivity of PPC gel.

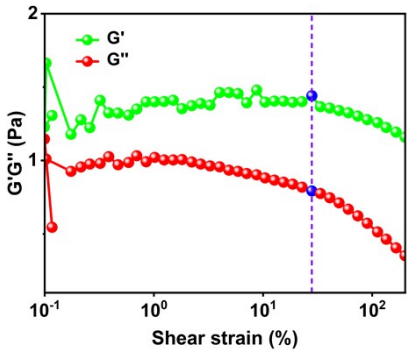

**Fig. S10** Strain sweep test of the PPC gel.

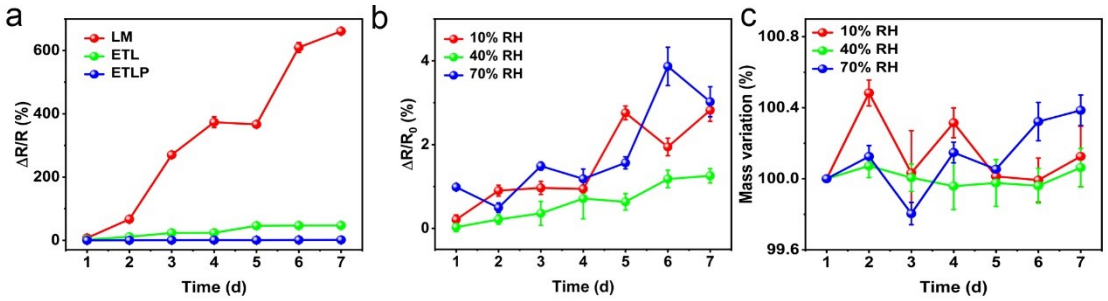


**Fig. S11** (a) Resistance changes of different samples after 7 d of aging. (b) Resistance changes of the ETLP electrode under different humidity conditions. (c) Mass variations of the ETLP electrode under different humidity conditions.

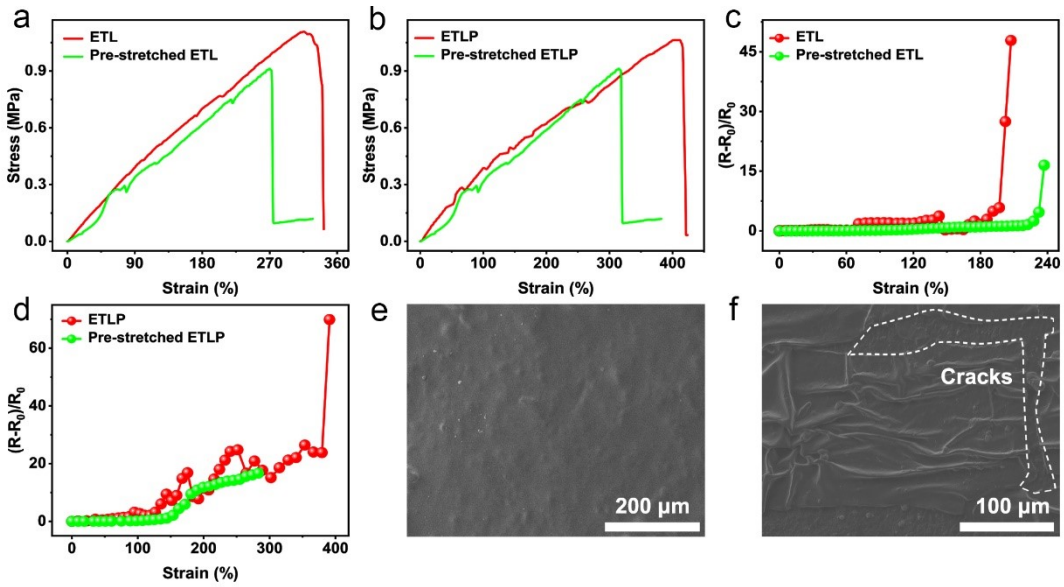


**Fig. S12** (a) Stress-strain curves of ETL electrode and pre-stretched ETL electrode. (b) Stress-strain curves of ETLP electrode and pre-stretched ETLP electrode. (c) Resistance change-strain curves of ETL electrode and pre-stretched ETL electrode. (d) Resistance change-strain curves of ETLP electrode and pre-stretched ETLP electrode. (e, f) Top-view SEM images: (e) ETLP electrode. (f) Pre-stretched ETLP electrode.

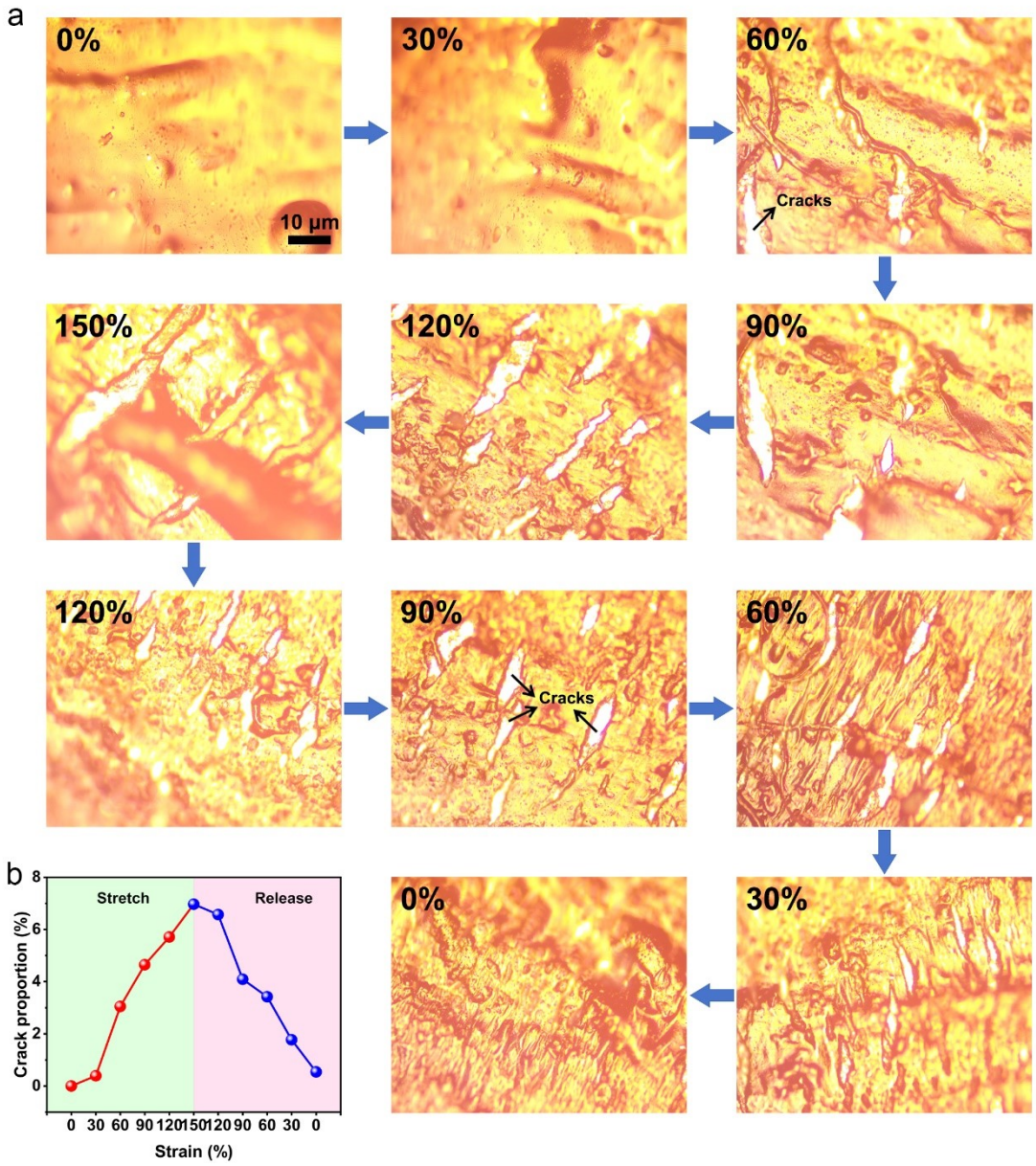


**Fig. S13** (a) Surficial optical images of ETLP electrode during stretch-release process. (b) Crack area proportion in ETLP electrode at different strains.

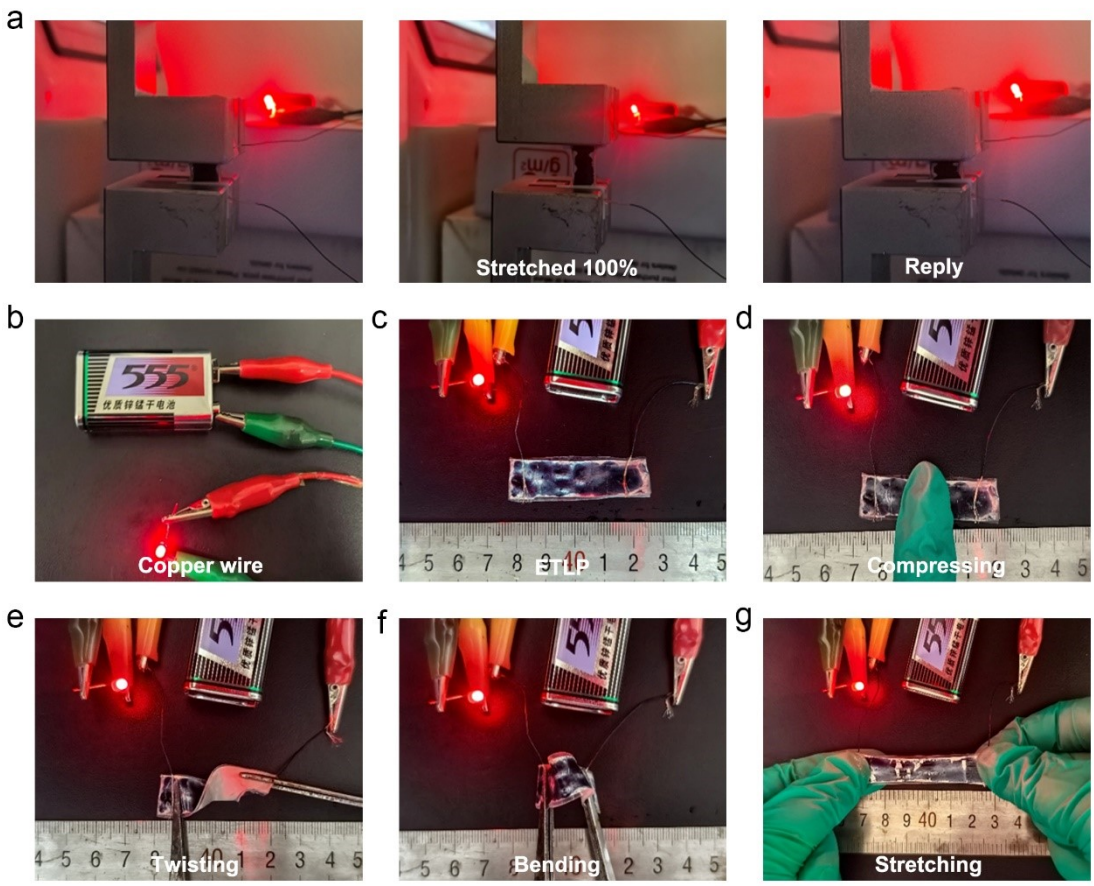


**Fig. S14** (a) Brightness variation of the LED when the ETLP electrode was stretched to 100%. (b) Photograph of an LED circuit connected with commercial copper wire. Photographs of the ETLP conductor under various mechanical deformations: (c) Initial state. (d) Compressing; (e) Twisting, (f) Bending, and (g) Stretching.

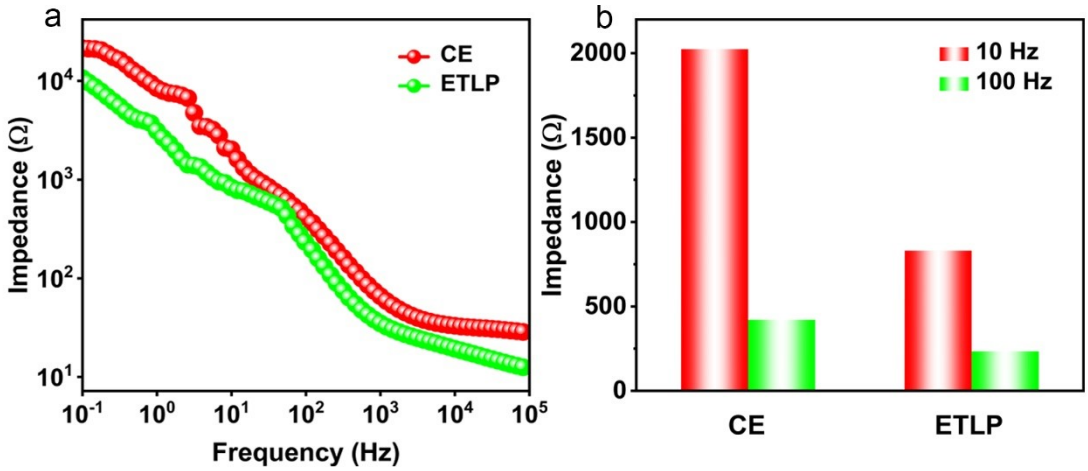


**Fig. S15** (a) Interfacial impedance comparison of CE and ETLP electrodes in PBS solution. (b) Interfacial impedance of CE and ETLP electrodes in PBS solution at 10 Hz and 100 Hz.

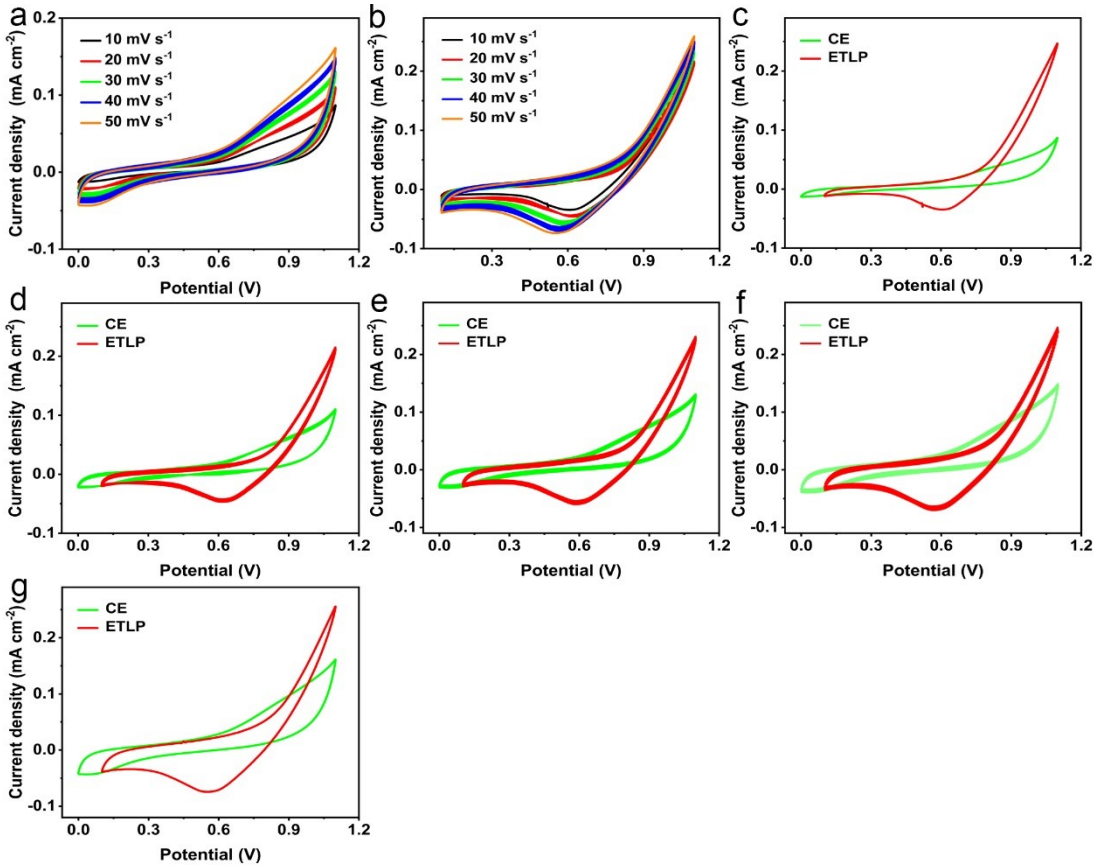


**Fig. S16** (a) CV curves of CE electrode in PBS solution. (b) CV curves of ETLP electrode in PBS solution. (c-g) CV curves of CE electrode and ETLP electrode in PBS solution at different scan rates: (c) 10 mV $s^{-1}$; (d) 20 mV $s^{-1}$; (e) 30 mV $s^{-1}$; (f) 40 mV $s^{-1}$; (g) 50 mV $s^{-1}$.

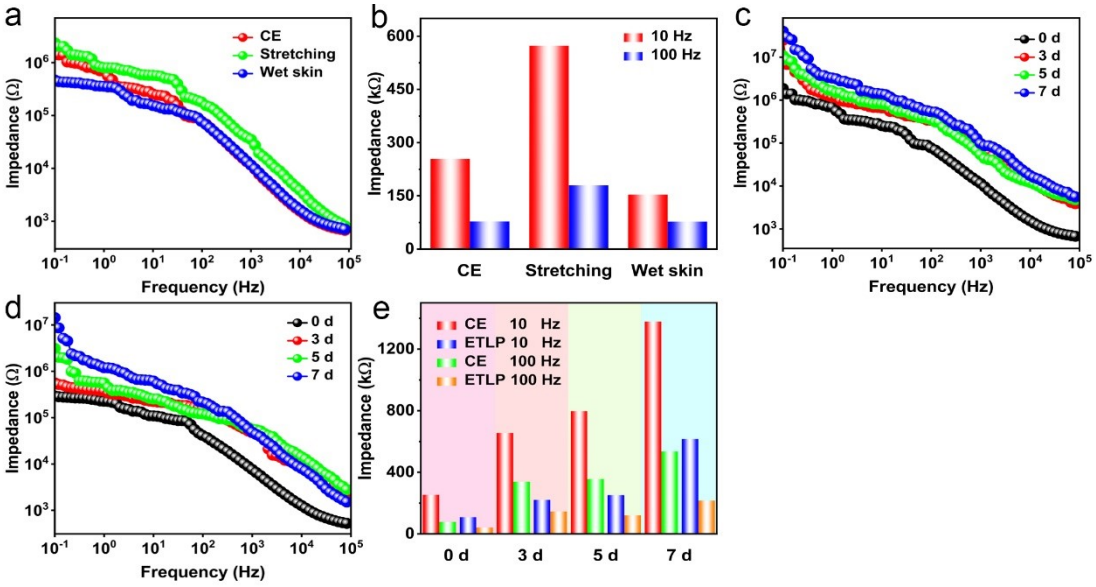


**Fig. S17** (a) Skin interfacial impedance comparison of CE electrode at different conditions. (b)

Interfacial impedance of CE electrode at different conditions at 10 Hz and 100 Hz. (c) Skin interfacial impedance comparison of CE electrode at 0, 3, 5, and 7 d. (d) Skin interfacial impedance comparison of ETLP electrode at 0, 3, 5, and 7 d. (e) Interfacial impedance of CE electrode and ETLP electrodes at 0, 3, 5, and 7 d at 10 Hz and 100 Hz.

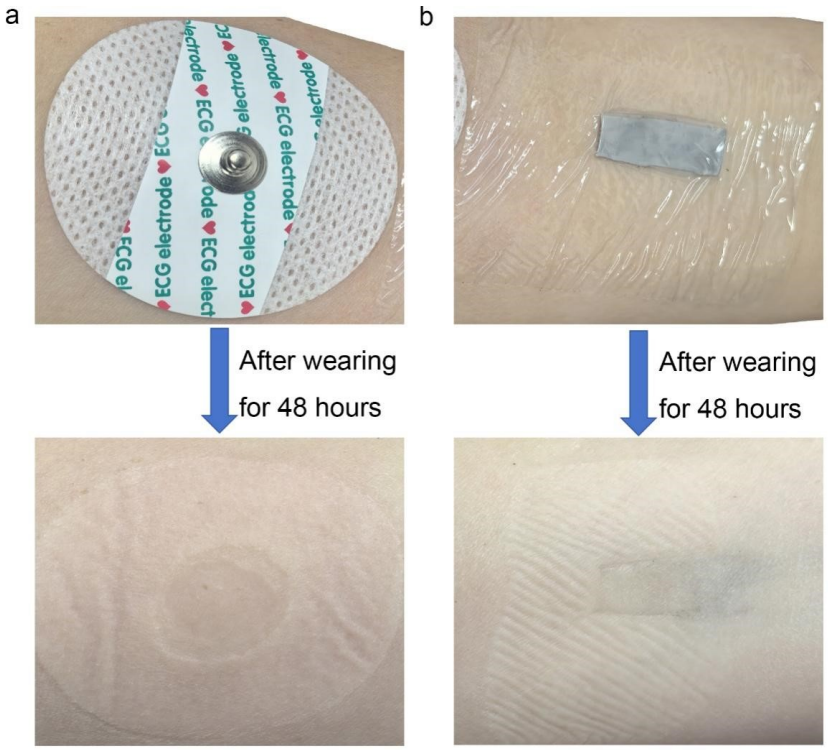


**Fig. S18** (a) Skin condition before and after 48 h of CE electrode attachment to human skin, (b) Skin condition before and after 48 h of ETLP electrode attachment to human skin.

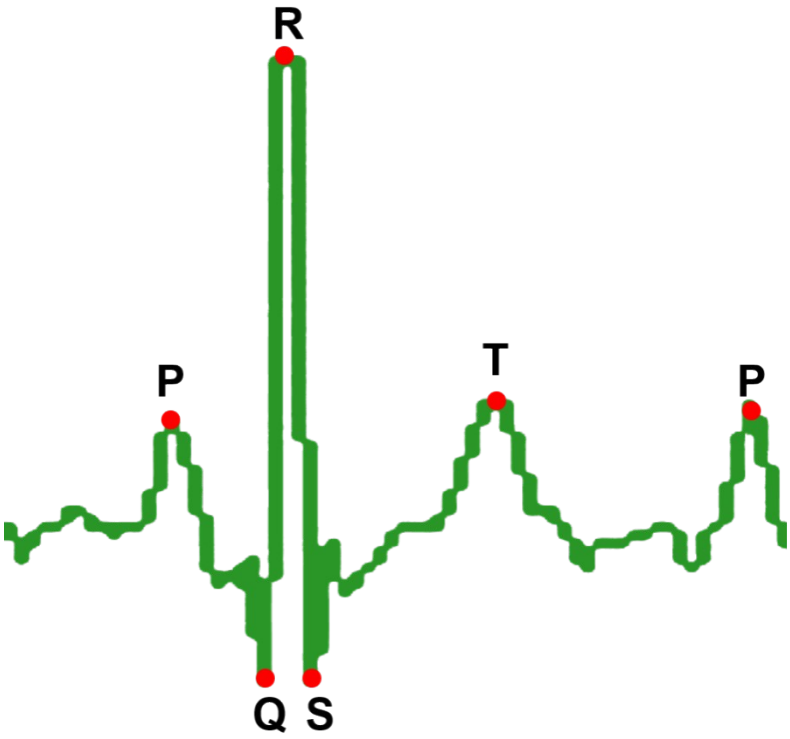


**Fig. S19** Schematic diagram of the 'PQRST' waves in an ECG signal.

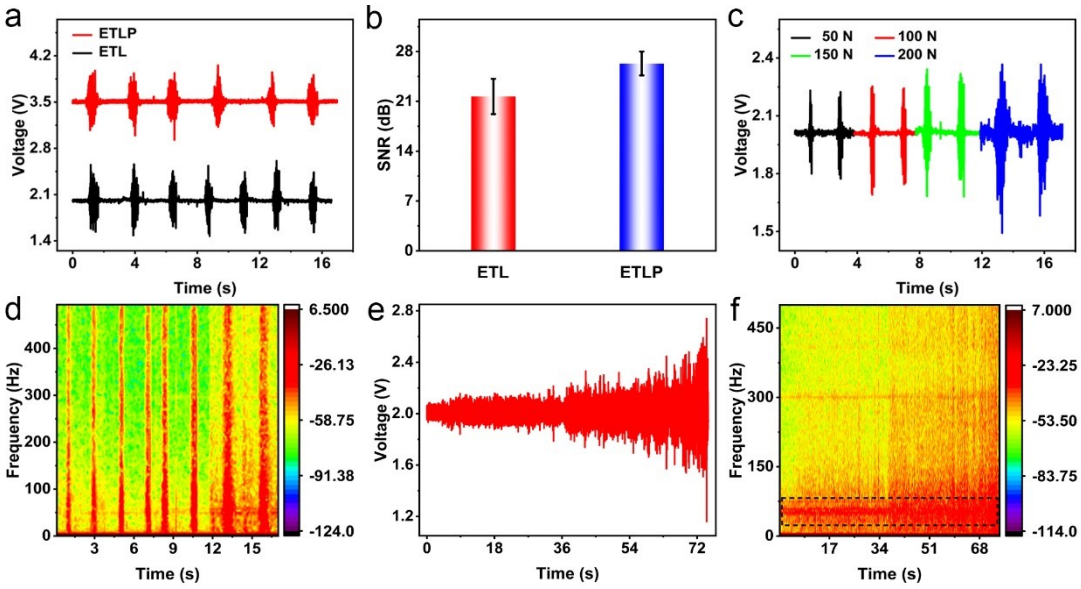


**Fig. S20** (a) Comparison of sEMG signals recorded by different electrodes during fist clenching. (b) Comparison of the SNR values of sEMG signals. (c) sEMG signals collected by the ETL electrodes at different grip forces. (d) Time-frequency spectrogram of the sEMG signals at different grip forces. (e) EMG signals of ETLP electrodes monitoring muscle fatigue stages. (f) Time-frequency spectrum of the sEMG signals at fatigue stages.

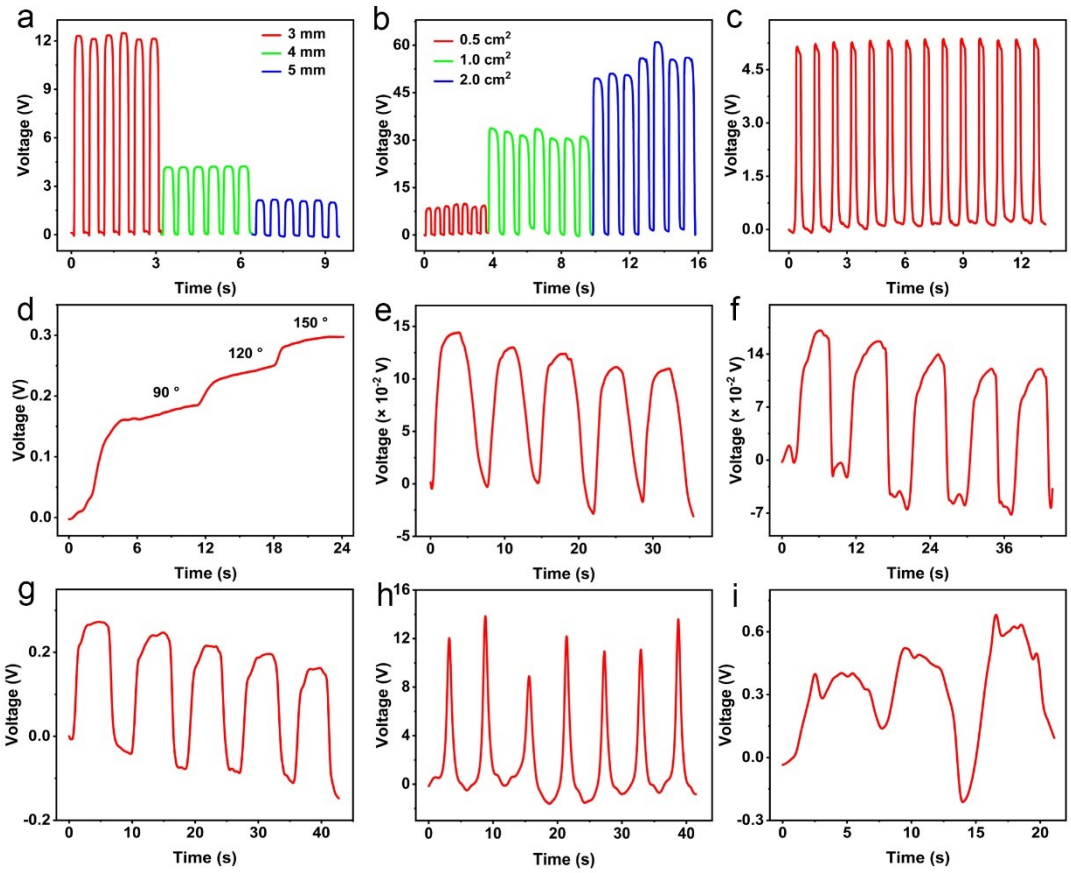


**Fig. S21** (a) The influence of Ecoflex thickness on output performance. (b) The influence of ETLP electrode area on output performance. (c) Finger pressing the TES repeatedly. (d) Finger bending angle increased from 90° to 150° and holding time. (e-h) The ETLP-based TES were attached to human joints: (e) Finger bending; (f) Wrist bending; (g) Elbow bending; (h) Knee bending. (i) Swallowing.

**Table S1.** Materials required for different $V_{PEDOT:PSS}/V_{PVA}$ ratios.

| Samples | PEDOT:PSS (mL) | PVA (7.4 wt%) (mL) | CA (mg) | Coating volume (mL) |
|---|---|---|---|---|
| ETLP-2:1 | 0.10 | 0.05 | 9 | 0.10 |
| ETLP-3:1 | 0.15 | 0.05 | 9 | 0.10 |
| ETLP-16:1 | 0.90 | 0.05 | 9 | 0.10 |

**Table S2.** Materials required for varied CA mass.

| Samples | PEDOT:PSS (mL) | PVA (7.4 wt%) (mL) | CA (mg) | Coating volume (mL) |
|---|---|---|---|---|
| ETLP-0 | 0.15 | 0.05 | 0 | 0.10 |
| ETLP-9 | 0.15 | 0.05 | 9 | 0.10 |
| TETLP-18 | 0.15 | 0.05 | 18 | 0.10 |
| ETLP-27 | 0.15 | 0.05 | 27 | 0.10 |

**Table S3.** Materials required for different coating volumes of 0.10-0.15 mL.

| Samples | PEDOT:PSS (mL) | PVA (7.4 wt%) (mL) | CA (mg) | Coating volume (mL) | |
|---|---|---|---|---|---|
| ETLP-0.05 | 0.15 | 0.05 | 9 | 0.05 | |
| ETLP-0.10 | 0.15 | 0.05 | 9 | 0.10 | This work |
| ETLP-0.15 | 0.15 | 0.05 | 9 | 0.15 | |

**Table S4.** Key parameters extracted from equivalent circuit modeling and Nyquist plot fitting.

| Samples | Rs (Ω) | CPE-T | CPE-P | Rct (Ω) |
|---|---|---|---|---|
| ETLP-2:1 | 695.4 | $3.4675\times10^{-6}$ | 0.40116 | 259110 |
| ETLP-3:1 | 24.8 | $5.4528\times10^{-7}$ | 0.60523 | 2136 |
| ETLP-16:1 | 49.1 | $8.6076\times10^{-7}$ | 0.5431 | 349010 |
| ETL | 755.5 | $1.670\times10^{-9}$ | 0.84865 | 36675 |
| PPC | 196.8 | $3.6208\times10^{-7}$ | 0.62541 | 141890 |

**Table S5.** Conductivity of different samples.

| Samples | EIS | Two-probe method |
|---|---|---|
| ETLP-3:1 (With Ecoflex) | 37.02 S $m^{-1}$ | 111.44 S $m^{-1}$ |
| ETLP-3:1 (Ecoflex removal) | 111.07 S $m^{-1}$ | 334.32 S $m^{-1}$ |
| ETL (With Ecoflex) | 1.94 S $m^{-1}$ | 122.61 S $m^{-1}$ |
| ETL (Ecoflex removal) | 5.19 S $m^{-1}$ | 335.13 S $m^{-1}$ |
| PPC | 104.48 S $m^{-1}$ | 3.01 S $m^{-1}$ |

**Table S6.** Comparison of the comprehensive properties in our work with those in published work.

| Substrate | Conductive materials | Conduction mechanism | Resistance changes at different strain | Interface impedance at 10 Hz (kΩ) | RMS noise (μV) | SNR noise (dB) | Capacitance response/recovery time | Ref. |
|---|---|---|---|---|---|---|---|---|
| AMPS/ MAEDS /AAM | $AgNO_3$ | Electron /ion | / | <100 | >20 | 21.83 | / | 1 |
| AM /gelatin /SA | PAAM /gelatin/SA | Electron | / | <60 | / | ~25 | / | 2 |
| SBS | cMOFs-b-CNTs/ILs | Electron /ion | >150 (400%) | 108.36 | 27.01 | 25.52 | / | 3 |
| PU/APDS /TEG /ZIF-67(NPs) | CNTs/CB | Ion | >2000 (600%) | / | 26.58 | 24.21 | / | 4 |
| TPU | APA/AA /SBMA | Electron | / | / | / | 21.4 | / | 5 |
| TPU | MXene | Electron /ion | ~175 (100%) | / | / | / | / | 6 |
| Ecoflex /PDMS | LM | Electron | 5 (100%) | / | / | / | / | 7 |
| AAM /N-THMA | PEDOT:PSS /ILs | Electron /ion | >60 (900%) | / | / | / | / | 8 |

| | | | | | | | | |
|---|---|---|---|---|---|---|---|---|
| Silicone | MXene | Electron/ion | >40 (2%) | / | / | / | / | 9 |
| Lithium BSL | PEDOT:PSS/ graphene /BSL | Electron /ion | >200 (40%) | >100 | 25.90 | / | / | 10 |
| TPU | Mxene /Ag NW | Electron /ion | >200 (15%) | / | / | / | / | 11 |
| Bandage | CNTs | Ion | ~450 (100%) | / | / | / | / | 12 |
| TPU | LM | Electron | / | / | / | / | 50 ms/60 ms | 13 |
| TPU | LM | Electron | ~0.4 (200%) | / | / | / | / | 14 |
| Ecoflex /TPU | LM/ PEDOT:PSS | Electron /ion | 2.1 (153.6%) | 108.8 | 24.30 | 24.65 | 5.6 ms/5.6 ms | This work |

AMPS: 2-acrylamido-2-methyl-1-propanesulfonic acid; $AgNO_3$: Silver nitrate; MAEDS: [2-(methacryloloxy) ethyl] dimethyl-(3-sulfopropyl); AAM: Acrylamide; PAAM: Polyacrylamide; SA: Sodium alginate; TEG: Tetraethyleneglycol; APDS: Bis-(4-aminophenyl) disulfide; NPs: Nanoparticles; CB: Carbon black; APA: Acryloyl phenylalanine; AA: Acrylic acid; SBMA: (3-sulfopropyl) ammonium hydroxide; PDMS: Polydimethy lsiloxane; THMA: (Tris(hydroxymethyl)methy) acrylamide; ILs: ionic liquids; BSL: Bis(trifluoromethanesulfonyl)imide.

**References**

1 C. He, J. Zhang, H. Wang, D. Wu, H. Zheng, Z. Guo, J. Xie, W. Zhu, M. Xie, J. Zhong, Y. Liu, Z. Li, G. Lin, Z. Peng, Adv. Funct. Mater., 2025, **34**, e09372.

2 X. Li, Y. Sun, S. Wang, G. Tian, T. Yang, L. Huang, Y. Ao, B. Lan, J. Zhang, T. Xu, Y. Liu, L.

Jin, W. Yang, W. Deng, Chem. Eng. J., 2024, **498**, 155195.

3 Y. Zhang, S. Wang, Y. Gao, M. Xia, A.T. Hoang, W. Guo, F. Wu, P. Liu, D. Cao, S. Zhao, G. Li, Y. Li, H. Cheng, J.H. Ahn, Adv. Funct. Mater., 2025, **35**, 1616-3028.

4 S. Zhao, Y. Zhou, M. Xia, Y. Zhang, S. Yang, A. Tuan Hoang, D. Cao, Y. Gao, Y. Lai, Chem. Eng. J., 2024, **489**, 151192.

5 K. Shen, Z. Lv, Y. Yang, H. Wang, J. Liu, Q. Chen, Z. Liu, M. Zhang, J. Liu, Y. Cheng, Adv. Mater., 2024, **37**, 1521-4095.

6 K. Yang, F. Yin, D. Xia, H. Peng, J. Yang, W. Yuan, Nanoscale, 2019, **11**, 9949-9957.

7 G. Li, M. Zhang, S. Liu, M. Yuan, J. Wu, M. Yu, L. Teng, Z. Xu, J. Guo, G. Li, Z. Liu, X. Ma, Nat. Electron., 2023, **6**, 154-163.

8 W. Wang, P. Guo, X. Liu, M. Chen, J. Li, Z. Hu, G. Li, Q. Chang, K. Shi, X. Wang, K. Lei, Adv. Funct. Mater., 2024, **34**, 1616-3028.

9 H. Wang, Y. Lin, C. Yang, C. Bai, G. Hu, Y. Sun, M. Wang, Y.-q. Lu, D. Kong, Nano Lett., 2024, **24**, 13405-13413.

10 Y. Zhao, S. Zhang, T. Yu, Y. Zhang, G. Ye, H. Cui, C. He, W. Jiang, Y. Zhai, C. Lu, X. Gu, N. Liu, Nat. Commun., 2021, **12**, 2041-1723.

11 Y. Shen, W. Yang, F. Hu, X. Zheng, Y. Zheng, H. Liu, H. Algadi, K. Chen, Adv. Compos. Hybrid Mater., 2022, **6**, 2522-0128.

12 L. Liu, D. Xiang, Z. Liu, X. Wang, Y. Li, C. Zhao, H. Li, B. Wang, P. Wang, J. Cheng, Y. Wu, Sens. Actuators, A., 2024, **368**, 115105.

13 Y. Chen, T. Feng, M. Peng, F. Qin. Adv. Fiber Mater., 2025, **7**, 633-644.

14 X. Wang, J. Liu, Y. Zheng, B. Shi, A. Chen, L. Wang, G. Shen. Sci China Mater, 2022 **65**, 2235-2243.